The Ni-doping Vanadium Borate Modification on $BiVO_4$ Photoelectrode Surface for Improving Charge Transfer and Photoelectrochemical Water Splitting

Dongbo Xu[a,b], Song Zhang[a], Cai Ning[c,*], Xiaoying Gao[a], Weidong Shi[a,c,*]

[a]School of Chemistry and Chemical Engineering, Jiangsu University, Zhenjiang 212013, PR China

[b]Jiangsu Key Laboratory of Advanced Structural Materials and Application Technology, Nanjing Institute of Technology, Nanjing 211167, PR China

[c]School of Environmental and Chemical Engineering, Jiangsu University of Science and Technology, Zhenjiang 212100, PR China

Corresponding author.

E-mail addresses: *cning@just.edu.cn*; *swd1978@ujs.edu.cn.*

1. Experiment

1.1 Preparation of Ni-VB/$BiVO_4$ photoelectrode

The pristine $BiVO_4$ photoelectrode was prepared according to the previous reports.[19] Furthermore, the nickel doped vanadium oxide (Ni-VO_x) was deposited on the $BiVO_4$ photoelectrode surface by using photo-electrodeposition method as follow: in 100 mL of deionized water, the VCl_3 and $Ni(NO_3)_2$ were configured with 10 mM and 0.1 mM, respectively. The prepared $BiVO_4$ photoelectrode, Ag/AgCl and Pt electrode were used as the working electrode, reference electrode and counter electrode, respectively. The voltage range was controlled to be in the range of -0.6~0.8 V (vs. RHE) for LSV test in 0.5 M potassium borate solution for 1

hour at the case of light illumination with AM 1.5G. Finally, the Ni-VO_x/$BiVO_4$ photoelectrode was obtained by rinsing with deionized water and dried in oven for 12 hours. Further on, the bimetallic Ni-VB/$BiVO_4$ photoelectrode was prepared also by using the photo-electrodeposition method as the same conditions of Ni-VO_x/$BiVO_4$ photoelectrode prepare process by using the Ni-VO_x/$BiVO_4$ photoelectrode as the working electrode.

1.2 Materials characterization

The crystalline structure of prepared photoelectrodes was analyzed by using X-Ray Diffractometer (XRD, Brooke D8) with Cu Kα radiation. The Raman spectroscopy was identified by using Thermo Fisher DXR spectrometer. The morphologies were characterized on scanning electronic microscopy (SEM, JEOL JSM-7800F), transmission electron microscopy and high resolution transmission electron microscope (TEM and HRTEM, FEI Tecnai F30) systems. The surface chemical state of elements was recorded on X-ray photoelectron spectroscopy (XPS, Thermo Fisher, ESCALAB 250). The Ultraviolet-visible diffuse reflectance (DRS) spectra were measured on a UV-3600 Plus (Shimadzu) spectrometer by using $BaSO_4$ as the reference. The density functional theory (DFT) calculations were performed using the Vienna Ab-initio Simulation Package (VASP) with projector-augmented wave (PAW) method. The $BiVO_4$ (1 2 1) surface was modeled as a 3×3×1 supercell with a 15 Å vacuum layer to avoid periodic interactions. The Ni-VB/$BiVO_4$ interface was constructed by replacing surface V atoms with Ni in the VB structure, and the oxygen vacancies (O_{vac}) were introduced by removing selected oxygen atoms. The detailed of DFT calculations were described in supporting information.

1.3 The measurements of PEC performances

All the PEC measurements were carried out in the 0.5 M KBi solution

(pH=9) by using an electrochemical workstation (CHI614) with a three-electrode system. A 300 W Xenon lamp was used as the solar light source and the illumination area of all photoelectrodes was controlled with 1 cm^2. In order to disperse the air in the solution, nitrogen gas was introduced for 30 min before the PEC tests. The workstation scan rate was controlled to be 50 mV/s and the photoelectrode samples were subjected to linear scanning voltammetry (LSV), stability (I-t) and Mott-Schottky tests. The charge injection ($\eta_{injection}$) and separation ($\eta_{separation}$) efficiency tests were performed with Na_2SO_3 as a hole scavenger. The photo-impedance (PEIS) was performed in the frequency range of 10^{-2}-10^{-6} and analyzed by fitting the clerk using analytical software (ZView).

2. Equations used in this work

E_{RHE} represents the converted potential vs. RHE. The value of $E^0_{Ag/AgCl}$ (saturated KCl) is 0.1976 V at 25 °C. $E_{Ag/AgCl}$ is the obtained potential vs. Ag/AgCl, and the pH of the electrolyte was 9;

Applied bias photon-to-current efficiency (ABPE) can be calculated using the following equation: [1]

$$APBE(\%) = \frac{J \times (1.23 - V_b)}{P_{total}} \quad (1)$$

Where J refers to the photocurrent density (mA cm^{-2}) obtained from the electrochemical workstation. V_b is the applied bias (vs RHE), and P_{total} is the total light intensity of AM 1.5 G (100 mW/cm^2).

The charge separation efficiency ($\eta_{separation}$) and injection ($\eta_{injection}$) efficiency of the pristine $BiVO_4$, V-NiO_x/$BiVO_4$, V-NiB/$BiVO_4$ can be calculated using the following equations: [2]

$$\eta_{separation} = \frac{J^{Na_2SO_3}}{J_{abs}} \quad (2)$$

$$\eta_{injection} = \frac{J^{Na_2SO_3}}{J_{max}} \quad (3)$$

Where J_{abs} is the photon adsorption rate expressed as the photocurrent density and $J^{Na_2SO_3}$ is the photocurrent densities in 0.5 M KBi with the addition of Na_2SO_3. J_{max} is the theoretical maximum photocurrent density of $BiVO_4$.

3. DFT Calculation Details:

All the spin-polarized first-principles calculations were performed using the Vienna Ab initio Simulation Package (VASP) [3] for the investigation of the oxygen evolution reaction (OER) on $BiVO_4$ and V-NiB/$BiVO_4$ heterogeneous catalysts. Interactions between ion cores and valence electrons were described using the Device Studio-integrated Projector Augmented-Wave method package (DS-PAW). The exchange-correlation functional was described using the generalized gradient approximation (GGA) with the Perdew-Burke-Ernzerhof (PBE) functional,[4] and the projector augmented wave (PAW) method[5] was used for the description of the electronic wavefunctions. A plane-wave cutoff energy of 400 eV was chosen, and the k-point sampling was performed using the Monkhorst-Pack (M-P) method[6] with a 3×2×1 grid to ensure adequate sampling of the first Brillouin zone. The forces were converged to within 0.02 eV/Å, and the total energy convergence criterion was set to 1×10^{-5} eV. During structural optimization, the lattice parameters of the unit cell were fixed, and a vacuum layer of 15 Å was introduced along the z-direction to minimize interactions between periodic images. A dipole correction was applied in the z-direction to account for long-range Coulomb interactions resulting from the periodic boundary conditions.[7] The DFT-D3 dispersion correction was included in all calculations.[8]

The materials considered in this study include the monoclinic $BiVO_4$ (121) surface and the possible VBO_3 (001) surface, with the lattice mismatch between the two phases constrained to be less than 5% to ensure the stability of the heterojunction interface. The lattice parameters of the heterojunction were optimized to 9.83 × 10.93 × 28 Å, ensuring low lattice mismatch and promoting a stable and efficient interface for catalytic activity.

For the oxygen evolution reaction (OER), the four-electron reaction steps were considered using the model developed by Nørskov et al.[9] The four-electron transfer process during the OER involves four reaction steps, including the formation of *OH, *O, and *OOH intermediates. The Gibbs free energy for each step was computed using the following equation:

$$\Delta G=\Delta E+\Delta ZPE-T\Delta S$$

where ΔE is the total energy difference between the initial and final states, ΔZPE is the difference in zero-point energy, T is the temperature 298.15 K, and ΔS is the change in entropy.

4. Supplemental data

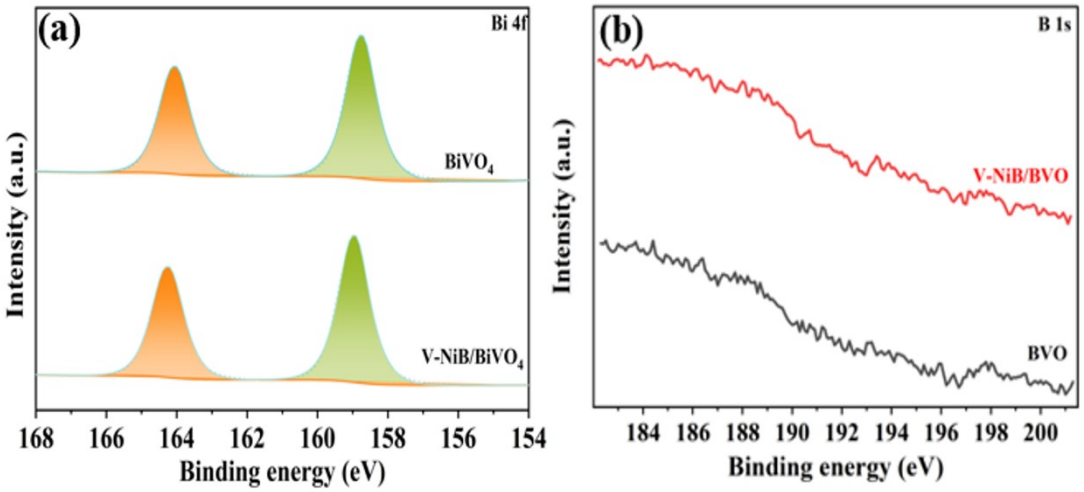

Fig. S1 The XPS of (a) Bi 4f and (b) V2p.

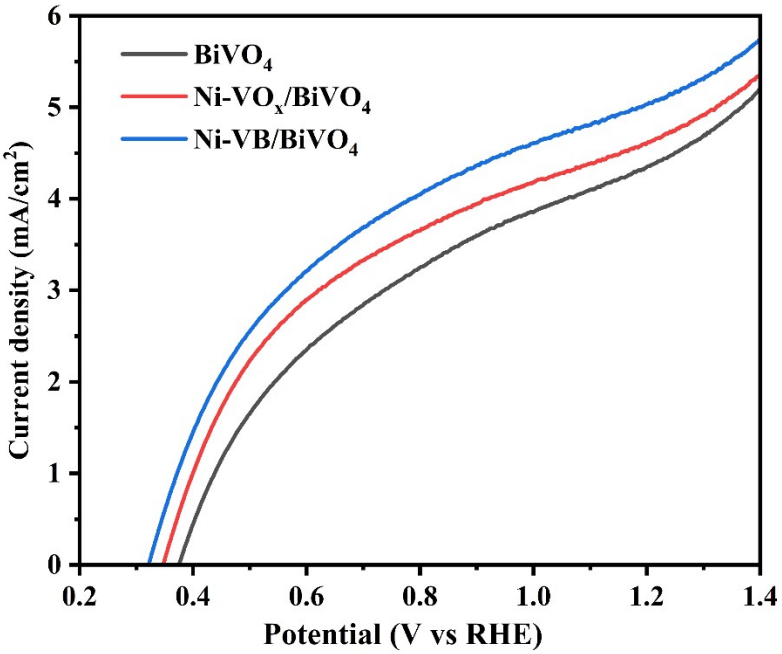

Fig. S2 The LSV tests of $BiVO_4$, Ni-VO_x/$BiVO_4$ and Ni-VB/$BiVO_4$ photoelectrodes with Na_2SO_3 sacrificial agent.

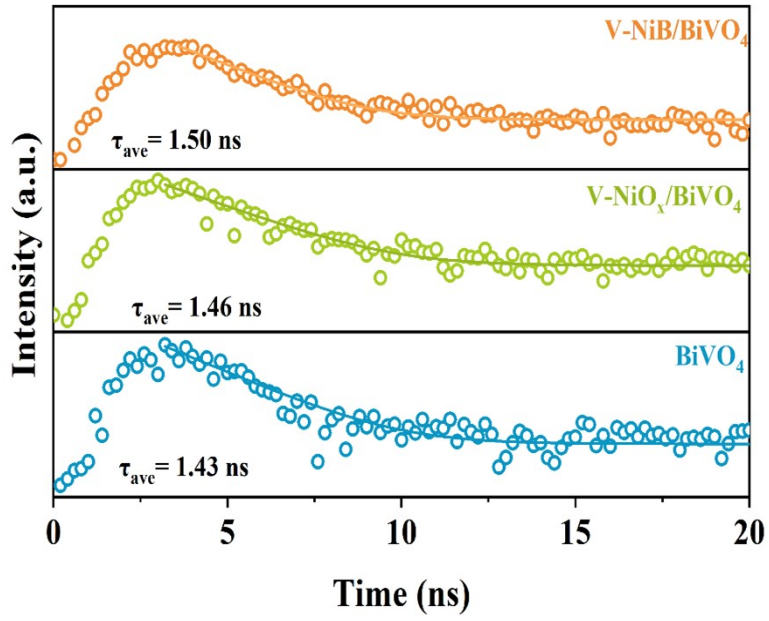

Fig. S3 The PL lifetime of $BiVO_4$, V-NiO_x/$BiVO_4$ and V-NiB/$BiVO_4$

samples.

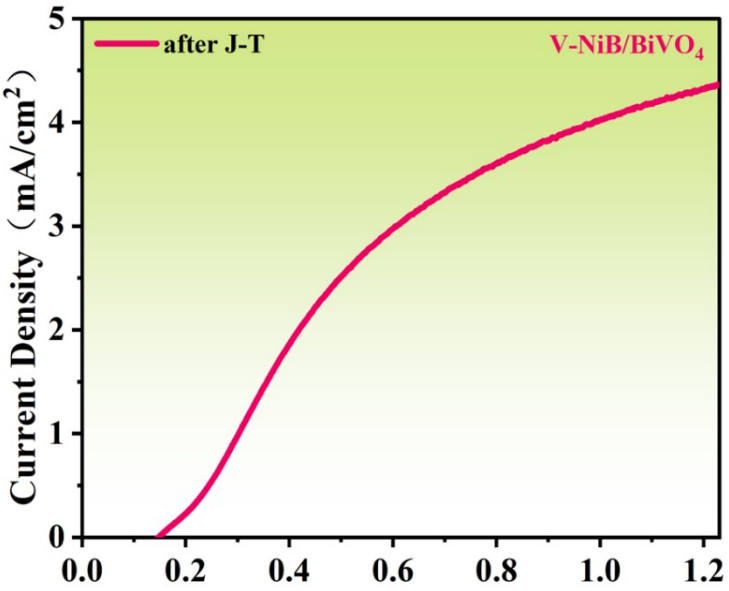

Fig. S4 The LSV curves of V-NiB/$BiVO_4$ electrodes after J-T.

Table S1. Comparison of PEC activities for $BiVO_4$ based photoelectrodes.

Photoelectrode	***J* (mA/cm^{-2}) AM 1.5G @1.23 V_{RHE}**	**Electrolyte**	**$BiVO_4$ based photoelectrode**	***J* (mA/cm^{-2}) AM 1.5G @1.23 V_{RHE}**	***J* ($BiVO_4$ based photoelectrode)/ *J* ($BiVO_4$)**	***J* (mA/cm^{-2}) AM 1.5G @1.23 V_{RHE} with sacrificial agent**	**Reference**
$BiVO_4$	1.7	0.5 M KPi	NiOOH/FeOOH /$BiVO_4$	4.2	2.5	4.0 (1.0 V_{RHE})	(10)
$BiVO_4$	*about 1.3	0.5 M KPi	NiOOH/FeOOH /N:$BiVO_4$	5	3.85		(11)
$BiVO_4$	0.67	0.1 M bicarbonate (CO_2)	Co-Ci/H,Mo:$BiVO_4$			5.1	(12)
$BiVO_4$		1 M KBi	$NiFeO_x$-Bi/$BiVO_4$	4.2			(13)
$BiVO_4$	1.4	0.5 M KBi	Co_4O_4 cubane/$BiVO_4$	5.1	3.65		(14)
$BiVO_4$	*about 1.45	0.4 M KBi	Fh/$BiVO_4$	4.87	3.3		(15)
$BiVO_4$/WO_3	*about 2	0.5 M KPi	NiOOH/FeOOH /$BiVO_4$/WO_3	5.5	2.75		(16)
$BiVO_4$	2.24	1 M KBi	$FeCoO_x$/$BiVO_4$	4.82	3.3		(17)
$BiVO_4$	*about 1.7	KBi+0.1 M V_2O_5	NiOOH/FeOOH /$BiVO_4$	4.8	2.82		(18)

$BiVO_4$	*about 1.1	0.2 M Na_2SO_4	β-FeOOH/$BiVO_4$	4.3	3.9		(19)
p-$BiVO_4$	3.9	0.5 M KPi	CoPi/etched p-$BiVO_4$	6.1	1.56		(20)
Mo-$BiVO_4$		1 M KPi	La:$BaSnO_3$/Mo:$BiVO_4$			5.15	(21)
$BiVO_4$	1.07	0.5 M KPi	NiOOH/Black P/$BiVO_4$	4.48	4.2		(22)
$BiVO_4$	*about 0.28	0.5 M Na_2SO_4+ 0.1 M KPi	Rh5%-$SrTiO_3$/$BiVO_4$	*about 0.71	2.5		(23)
$BiVO_4$	1.6	0.5 M KBi	B-$BiVO_4$	3.5	2.2	*about 4.8	(24)
$BiVO_4$	1.75	1 M KBi + NaOH	$NiFeO_x$/$BiVO_4$	5.54	3.2	6.02	(25)
$BiVO_4$	2.96	1 M KBi	FeOOH/etched-NiOOH/$BiVO_4$	5.43	1.83	5.8	(26)
$BiVO_4$	2.3	1 M KBi	NiFe(Y) LDH/$BiVO_4$	5.2	2.26	5.25	(27)
$BiVO_4$	2.1	0.5 M KBi	NiFeOOH/$BiVO_4$	5.8	2.76		(28)
$BiVO_4$	0.6	0.1 M KPi	carbon spheres-$BiVO_4$	*about 2.22	3.7		(29)

$BiVO_4$	1.34	1 M KBi	photo-activated -Pt:$BiVO_4$	5.45	4.1	5.5	(30)
$BiVO_4$	2.1	0.5 M KBi	N:$NiFeO_x$/$BiVO_4$	6.4	3.0		(31)
$BiVO_4$	1.8	1 M KBi	Co^{2+} and cucurbit[5]uril (Co@CB[5])/$BiVO_4$	4.8	2.7		(32)
$BiVO_4$	0.85	0.5 M Na_2SO_4	$Co(OH)_x$-Ag/$BiVO_4$	3.95	4.64	*about 4.7	(33)
$BiVO_4$	*about 1.9	0.1 M KPi	Co-Pi/N-$BiVO_4$	3.7	2		(34)
Black P QDs/$BiVO_4$	1.7	0.5 M KPi	Black P QDs/E-etched $BiVO_4$	3.32	2		(35)
Mo-$BiVO_4$	3.82	1 M KPi	FeNiOOH-LGCDs-PHGs-Mo-$BiVO_4$	6.08	1.6		(36)
$BiVO_4$/nickel foam (NF)	1	0.5 M Na_2SO_4	A-$CoMoO_{4-x}$/$BiVO_4$/NF	3.5	3.5	5.2	(37)
$BiVO_4$	1.43	0.5 M KBi	Co-agZIF-62(Zn)/NiO/$BiVO_4$	5.34	3.73		(38)

$BiVO_4$	1.3 (Na_2SO_4 solution)		NiB (borate)-$BiVO_4$ (Na_2SO_4+borate)	6		*about 6.5	(39)
$BiVO_4$	1.63	1 M KBi	$VO_x/BiVO_4$	6.29	3.85	6.58	(40)
$BiVO_4$	1.9	0.5 M KBi	NiCoFe-Bi/CuSCN/$BiVO_4$	5.6	2.95	*about 6.25	(41)
$BiVO_4$	1.57	0.5 M KBi	FeCoNiMoGrOOH/$BiVO_4$	5.23	3.3		(42)
$BiVO_4$	1.61	0.5 M KBi	$[FeCl_4]$PTh/$BiVO_4$	4.72	2.9	*about 5.9	(43)
$BiVO_4$	*about 1.85	1 M KBi	O_v-$BiVO_4$/MIL-101	5.91	about 3.2		(44)
$BiVO_4$	1.2	1 M KBi	Ni-VB/$BiVO_4$	4.8	4	7.5	This work

*about: The authors didn't show the detailed photocurrent densities in published papers, these numerical values were from the figures of photocurrent densities with approximate.

Tab. S2 The PEIS fitting parameters of $BiVO_4$, Ni-VO_x/$BiVO_4$ and Ni-VB/$BiVO_4$ samples.

Sample	R_S	R_{Ct}
$BiVO_4$	15.97	632.7
V-NiO_x/$BiVO_4$	16.21	390.5
V-NiB/-$BiVO_4$	16.24	177.4

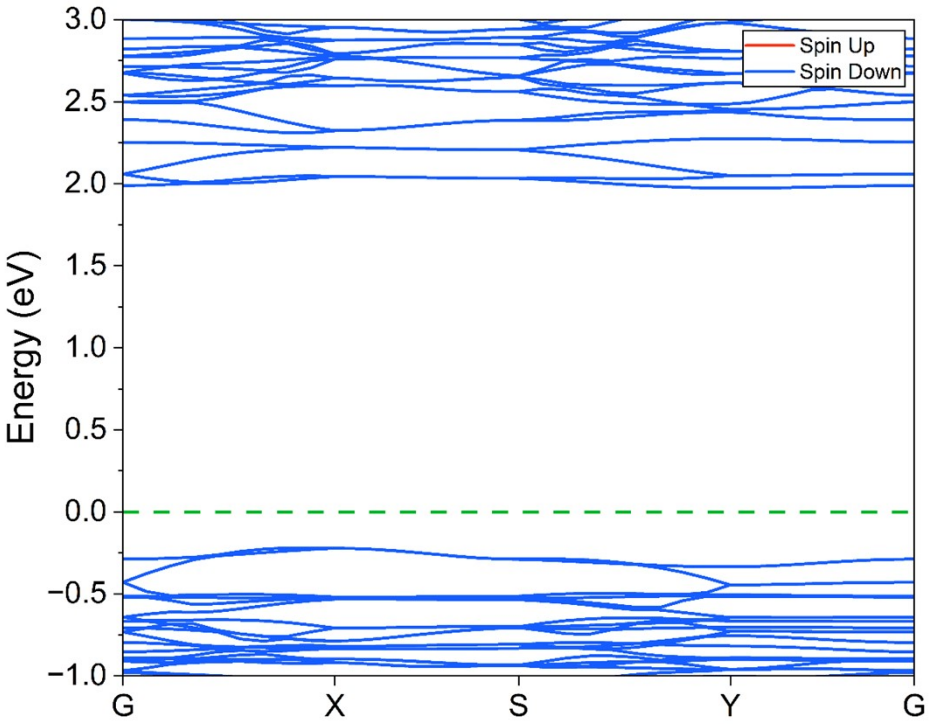

Fig. S5 The band structure DFT calculation of pristine $BiVO_4$.

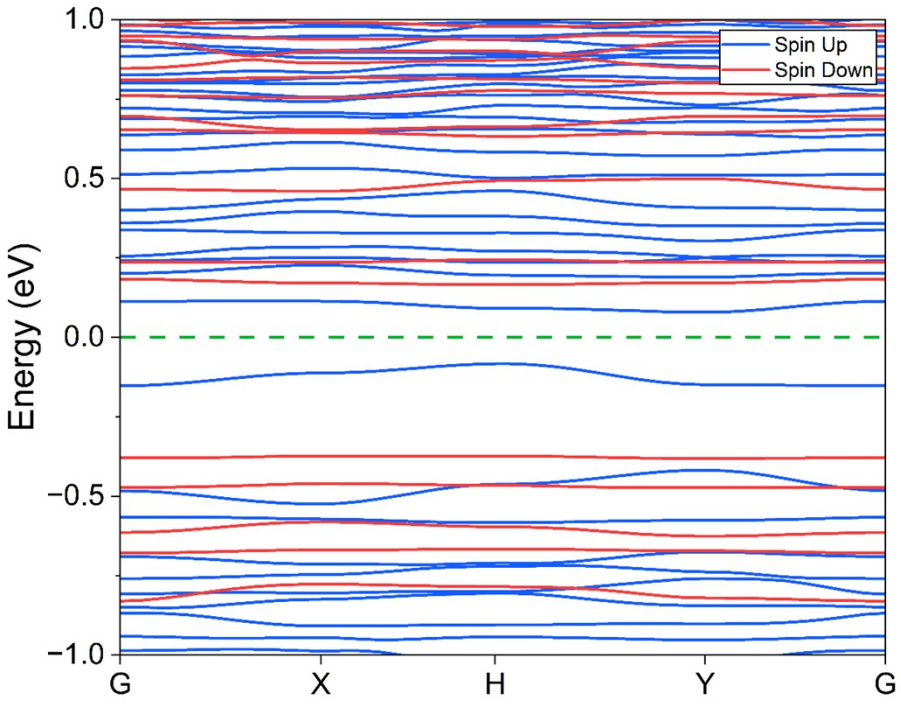

Fig. S6 The band structure DFT calculation of VB/$BiVO_4$.

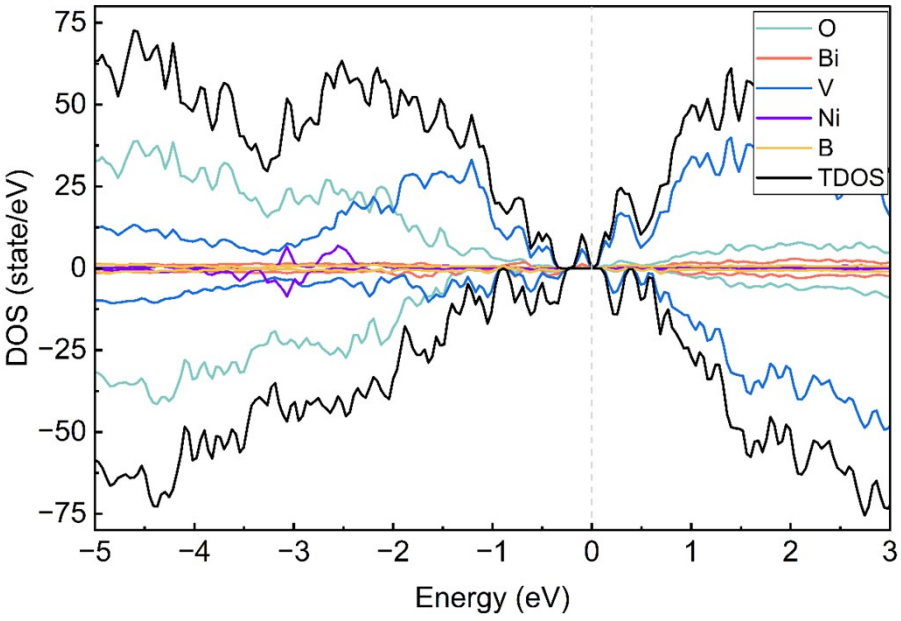

Fig. S7 The DOS calculation of Ni-VB/$BiVO_4$.

References

[1] K. Li, Y. Yang, Y. Feng, S. Ajmal, I. Nabi, L. Zhang. Efficiently complete degradation of 2,4-DCP using sustainable photoelectrochemical

reduction and sequential oxidation method. Chem. Eng. J., 2019, 378, 122191.

[2] F. Li, W. Zhao, D. Y. C. Leung. Enhanced photoelectrocatalytic hydrogen production via Bi/$BiVO_4$ photoanode under visible light irradiation. Appl. Catal. B Environ., 2019, 258, 117954.

[3] Kresse, G.; Hafner, J. Ab initio molecular dynamics for liquid metals. Physical Review B, 1993, 47, 558-561.

[4] Perdew, J. P.; Burke, K.; Ernzerhof, M. Generalized Gradient Approximation Made Simple. Physical Review Letters, 1996, 77, 3865-3868.

[5] Blöchl, P. E. Projector augmented-wave method. Physical Review B, 1994, 50, 17953-17979.

[6] Monkhorst, H. J.; Pack, J. D. Special points for Brillouin-zone integrations. Physical Review B, 1976, 13, 5188-5192.

[7] Neugebauer, J.; Scheffler, M. Adsorbate-substrate and adsorbate-adsorbate interactions of Na and K on the (111) surface of Au and Pt. Physical Review B, 1992, 46, 16067-16080.

[8] Grimme, S.; et al. Dispersion correction for density functional theory calculations of molecular complexes. Journal of Computational Chemistry, 2010, 31, 2872-2880.

[9] Nørskov, J. K.; et al. Electrocatalysis in the oxygen reduction reaction. Nature Materials, 2008, 7, 951-956.

[10] Science 2014, 343, 990-994.

[11] Nat. Commun., 2015, 6, 8769.

[12] ACS Nano 2015, 9, 11820-11829.

[13] Adv. Energy Mater., 2016, 6, 1501645.

[14] Angew. Chem. Int. Ed., 2017, 56, 6911-6915.

[15] ACS Catal., 2017, 7, 1868-1874.

[16] Nano Lett., 2017, 17, 8012-8017.

[17] Adv. Funct. Mater., 2018, 28, 1802685.

[18] Nat. Energy, 2018, 3, 53-60.

[19] Angew. Chem. Int. Ed., 2018, 57, 2248-2252.

[20] Energ. Environ. Sci., 2018, 11, 1299-1306.

[21] Nat. Commun., 2019, 10, 2609.

[22] Nat. Commun., 2019, 10, 2001.

[23] Adv. Funct. Mater., 2019, 29, 1902101.

[24] Angew. Chem. Int. Ed., 2019, 58, 19027.

[25] Adv. Mater., 2020, 32, 2001385.

[26] Angew. Chem. Int. Ed., 2020, 59, 6213-6218.

[27] ACS Catal., 2020, 10, 10570-10576.

[28] Angew. Chem. Int. Ed., 2020, 59, 18990-18995.

[29] ACS Catal., 2020, 10, 13031-13039.

[30] Adv. Energy Mater., 2021, 11, 2102384.

[31] Nat. Commun., 2021, 12, 6969.

[32] Angew. Chem. Int. Ed., 2021, 60, 1976-1985.

[33] Adv. Energy Mater., 2021, 11, 2100405.

[34] Adv. Funct. Mater., 2021, 31, 2008656.

[35] Energ. Environ. Sci., 2022, 15, 672-679.

[36] Adv. Mater., 2022, 34, 2201140.

[37] ACS Catal., 2022, 12, 1686-1696.

[38] Angew. Chem. Int. Ed., 2023, 62, e202306420.

[39] Sci. Adv., 2023, 9, eade4589.

[40] Angew. Chem. Int. Ed., 2023, 62, e202217346.

[41] Adv. Energy Mater., 2024, 14, 2304223.

[42] Adv. Funct. Mater., 2024, 34, 2403948.

[43] Nat. Commun., 2024, 15, 2023.

[44] Adv. Mater., 2025, 37, 2417589.